

# Combining Teacher-Student with Representation Learning: A Concurrent Teacher-Student Reinforcement Learning Paradigm for Legged Locomotion

Hongxi Wang\*, Haoxiang Luo\*, Wei Zhang and Hua Chen

**Abstract**—Thanks to the explosive developments of data-driven learning methodologies recently, reinforcement learning (RL) emerges as a promising solution to address the legged locomotion problem in robotics. In this manuscript, we propose a novel *concurrent* teacher-student reinforcement learning architecture for legged locomotion over challenging terrains, based only on proprioceptive measurements in real-world deployment. Different from conventional teacher-student architecture that trains the teacher policy via RL and transfers the knowledge to the student policy through supervised learning, our proposed architecture trains teacher and student policy networks concurrently under the reinforcement learning paradigm. To achieve this, we develop a new training scheme based on conventional proximal policy gradient (PPO) method to accommodate the interaction between teacher policy network and student policy network. The effectiveness of the proposed architecture as well as the new training scheme is demonstrated through extensive indoor and outdoor experiments on quadrupedal robots and point-foot bipedal robot, showcasing robust locomotion over challenging terrains and improved performance compared to two-stage training methods.

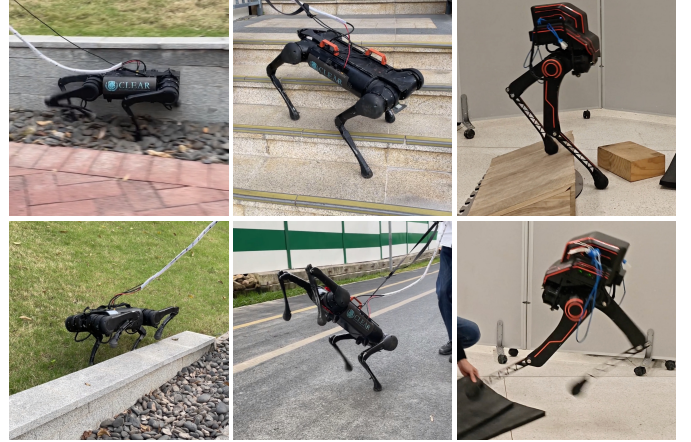


Fig. 1: Our training method enables legged robots of various sizes and configurations to achieve robust and agile locomotion across challenging real-world terrains, while also possessing exceptional capabilities to withstand strong external disturbances.

## I. INTRODUCTION

Locomotion is one of the most important skills for legged robots, which enables them to traverse complicated terrains to accomplish various tasks [1]–[7]. Due to the complicated contact interaction with the uneven terrain and the inherent nonlinear and hybrid dynamics for legged locomotion, the locomotion controller synthesis problem is widely acknowledged to be challenging [8]. Recently, reinforcement learning-based methods have been shown to be a promising solution to legged locomotion and have achieved remarkable results [9]–[13].

Nowadays, the so-called teacher-student paradigm is one of the most widely adopted and studied methodology for achieving legged locomotion with reinforcement learning [10], [14], [15]. In such a paradigm, a teacher policy having full access to all information (*privileged*) related to locomotion (e.g., terrain details, contact information, accurate inertial parameters, etc.) is trained by reinforcement learning. Then, a student policy that operates purely with proprioceptive feedback is trained by supervised learning to imitate the behavior of trained teacher policy. This approach allows for efficient learning and sim-to-real transfer of the policy to real-world where the robot operates with only proprioception. Such a methodology has been widely extended and been shown effective in enabling

various legged robots to achieve locomotion in complex terrains [10], [15], [16]. [15] integrates teacher-student learning with Adversarial Motion Priors (AMP) to enable quadruped to learn natural and robust locomotion. [16] leverages the advances in rapid motor adaptation for quadruped locomotion proposed originally in [10], and expands them to humanoid robots. Similar training paradigm has also been shown capable of addressing other challenging locomotion tasks with richer inputs including exteroceptive measurements [17]–[21].

Different from the teacher-student paradigm, representation learning integrates dynamics learning to enhance legged locomotion [22], [23]. DreamWaQ [22] leverages learned representations through variational autoencoders (VAE) to improve legged locomotion performance. Hybrid Internal Model [23] treats external states like terrain conditions as disturbances. It learns representations through contrastive learning, which pulls close the representations generated from historical sequence of observations and future observations. A common characteristic of these methodologies is the use of a regression objective for state representation, which requires the neural network to match the targets accurately.

Most of the aforementioned RL-based strategies are validated with quadruped platforms over challenging terrains. Extensions of these methods to bipedal robots have not been fully investigated. [24] achieved the sim-to-real transfer of a RNN policy for bipedal walking on flat ground. [25] employs a terrain randomization approach to implement proprioceptive controllers for bipedal robots involved in climbing and descending stairs. However, these methods employ vanilla reinforcement learning to train policy networks while overlooking

\*: these authors contributed equally.

Hongxi Wang, Haoxiang Luo and Wei Zhang are with School of System Design and Intelligent Manufacturing (SDIM), Southern University of Science and Technology, Shenzhen, China. Emails: {12332640, 12232312}@mail.sustech.edu.cn, zhangw3@sustech.edu.cn

Hua Chen is with Zhejiang University-University of Illinois Urbana-Champaign Institute (ZJUI), Haining, China. Email: huachen@intl.zju.edu.cn

the full utilization of privileged information, suggesting that there is considerable room to enhance the blind locomotion capabilities of bipedal robots.

In this work, we explore the mechanism for systematically integrating the information from the teacher strategy with that from the student strategy. To this end, we propose a concurrent teacher-student learning architecture for legged locomotion, which philosophically combines the teacher-student paradigm with the core of representation learning and embodies the training of teacher and student policies concurrently. Based on teacher-student paradigm, we develop a variant of the PPO training algorithm to incorporate the iterative training of the teacher and student policy to ensure convergence of the overall training process. We validate our approach with multiple hardware platforms including quadrupeds of different sizes and with a more challenging, underactuated bipedal robot with point feet. Furthermore, robots have demonstrated the ability to navigate through challenging terrains and against external disturbances.

The contributions of this work are summarized as follows. First, we develop a novel concurrent teacher-student reinforcement learning architecture that integrates standard teacher-student paradigm and representation learning to exploit the interplay between teacher and student networks to enhance the reinforcement learning performance. Second, we show that the proposed architecture exhibits significant generalizability and adaptability across different locomotion problems with different hardware platforms with minimal modifications. Third, extensive hardware experimental results with various hardware platforms, including quadrupeds and point-foot biped, are demonstrated, achieving robust locomotion over challenging terrains in both indoor and outdoor environments.

## II. CONCURRENT TEACHER-STUDENT REINFORCEMENT LEARNING FOR LEGGED LOCOMOTION

An overview of the proposed concurrent teacher-student reinforcement learning architecture for legged locomotion is shown in Fig. 2. In this section, we formulate our problem and develop the proposed architecture.

### A. Legged Locomotion Problem and Reinforcement Learning

In essence, legged locomotion focuses on finding the appropriate joint torque commands for all actuated joints of the robots given the sensory measurements. Under the assumption of only having accessibility to proprioceptive measurements from IMU and joint encoders, the legged locomotion dynamics can be formulated as the following infinite-horizon partially observable Markov decision process (POMDP), defined by the tuple  $\langle \mathcal{S}, \mathcal{A}, \mathcal{O}, T, \Omega, R \rangle$ , where  $\mathcal{S} \subset \mathbb{R}^n$  is the set of full state including all dynamic information of legged robot and environment around,  $\mathcal{A} \subset \mathbb{R}^m$  is the set of action,  $\mathcal{O} \subset \mathbb{R}^o$  is the set of observation,  $T(s', s, \mathbf{a}) = p(s'|s, \mathbf{a})$  is the state transition function,  $\Omega(\mathbf{o}, s, \mathbf{a}) = p(\mathbf{o}|s, \mathbf{a})$  is the observation function and  $R(s, \mathbf{a}, s')$  is the reward function. Our goal is to find the optimal policy  $\pi^*$  to maximize the expected

discounted return over the trajectory:

$$J(\pi) = \mathbb{E}_\pi \left[ \sum_{t=0}^{\infty} \gamma^t R(\mathbf{s}, \mathbf{a}, \mathbf{s}') \right] \quad (1)$$

with discounting factor  $\gamma \in [0, 1]$ .

**State Space:** We denote by  $\mathbf{o}_t$  the observation and  $\mathbf{s}_t$  the state at time  $t$ . The proprioceptive observation  $\mathbf{o}_t \in \mathbb{R}$  consists of angular velocity, gravity vector in the base frame of the robot, joint positions and velocities, command, and previous actions. The command consists of the desired velocity  $v_x^{\text{cmd}}, v_y^{\text{cmd}}$  and the angular velocity  $\omega_z^{\text{cmd}}$  in the base frame. The full state  $\mathbf{s}_t$  consists of proprioceptive observation  $\mathbf{o}_t$ , base linear velocity  $\mathbf{v}_t \in \mathbb{R}^3$ , terrain height samples  $i_t \in \mathbb{R}$  and other privileged information including feet contact forces, joint torques and acceleration of joints.

**Action Space:** For each actuated joint, the action  $\mathbf{a}_t \in \mathbb{R}$  represents the angular deviation of the robot's joint relative to its nominal position. Hence, the robot's joint PD controller reference is

$$\mathbf{q}_t^{\text{ref}} = \mathbf{q}^{\text{nominal}} + K \mathbf{a}_t \quad (2)$$

with some scale  $K$ .

### B. Concurrent Teacher-Student Network Architectures

To learn the optimal policy, the robot needs to infer its current state  $\mathbf{s}_t$  from the available observation  $\mathbf{o}_t$ . It is in general impossible to infer the actual state from a single observation, due to the partial observability of the environment. Thus, the inference problem  $p(\mathbf{s}_t | \mathbf{o}_t, \mathbf{o}_{t-1}, \dots, \mathbf{o}_{t-n})$  requires the historical sequence of observation. Recent works have leveraged variational autoencoder (VAE) or teacher-student learning to implicitly infer state- or task-relevant information. We integrated the advantages of both approaches and employed Proximal Policy Optimization (PPO) for training.

We train the teacher and student policy concurrently by dividing parallel agents into two groups named teacher group and student group, then employing the asymmetric actor-critic framework shown in Fig. 2. Agents in two groups are both trained using proximal policy optimization (PPO) while they share the same policy network  $\pi_\theta$  and critic network  $V_\phi$  designed as the Multi-Layer Perceptron (MLP) with Exponential Linear Unit (ELU) activation. The policy network outputs action  $\mathbf{a}_t$  given proprioceptive observation  $\mathbf{o}_t$  and latent representation  $\mathbf{z}_t \in \mathbb{R}^{32}$ , which were generated by the precedent encoder designed as MLP with ELU activation. The latent representation  $\mathbf{z}_t$  is mapped onto a unit hypersphere with a  $\mathcal{L}_2$ -normalization. The critic network estimates the state value given state  $\mathbf{s}_t$  and latent representation  $\mathbf{z}_t$ .

Throughout this manuscript, we use superscripts  $(\cdot)^t$  and  $(\cdot)^s$  to indicate teacher group and student group, respectively. Agents in teacher group have access to full state  $\mathbf{s}_t$  while they utilize privileged encoder  $E_\theta^t$  to encode state  $\mathbf{s}_t^t$  into latent representation  $\mathbf{z}_t^t$ . Agents in the student group only have access to proprioceptive observation, allowing policies to be deployed in real environments. Proprioceptive encoder  $E_\theta^s$  is leveraged to encode observation sequence  $\mathbf{o}_{t-H:t}^s = [\mathbf{o}_t^s, \dots, \mathbf{o}_{t-H}^s]^T$  into latent representation  $\mathbf{z}_t^s$  similar to privileged encoder.

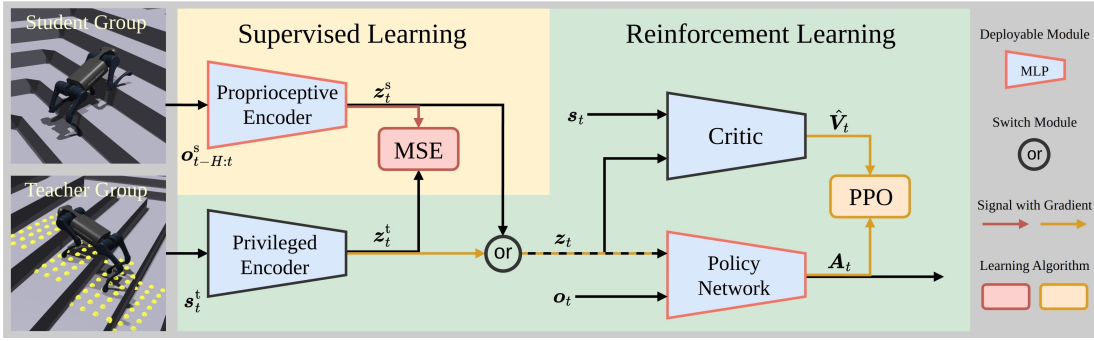


Fig. 2: Overview of the learning framework. The teacher and student policies are trained concurrently using PPO within an asymmetric actor-critic framework. Agents in both groups share the same policy and critic networks, with actions determined by observations and latent representations from either privileged or proprioceptive encoder. The privileged encoder is trained via policy gradient, while the proprioceptive encoder undergoes supervised learning to minimize reconstruction loss.

The latent representation  $z_t$  is generated from the privileged encoder or the proprioceptive generator, which guides the policy network to produce specific actions for various terrains and scenarios. The privileged encoder and policy network is trained through policy gradient to maximize the expected discounted return, while the proprioceptive encoder is trained through supervised learning to minimize the reconstruction loss between outputs of proprioceptive encoder and privileged encoder. More details on each network are shown in Table I.

TABLE I: Network Architectures

Module	Notation	Inputs	Outputs
Privileged Encoder	$E_{\theta^t}$	$\mathbf{s}_t^t$	$\mathbf{z}_t^t$
Proprioceptive Encoder	$E_{\theta^s}$	$\mathbf{o}_{t-H:t}^s$	$\mathbf{z}_t^s$
Policy Network	$\pi_{\theta}$	$\mathbf{o}_t, \mathbf{z}_t$	$\mathbf{a}_t$
Critic	$V_{\phi}$	$\mathbf{s}_t, \mathbf{z}_t$	$\hat{V}_t$

### C. Training Pipeline

Due to the structural change of the overall architecture and the way we exploit the information from the teacher and student groups, the conventional training process does not apply directly and hence needs to be adjusted. The training process of proposed concurrent teacher-student pipeline is shown in Algorithm 1. Since agents are divided into two groups, the Monte-Carlo approximation of PPO-Clip objective functions of each group  $L^t(\theta, \theta^t)$ ,  $L^s(\theta)$  is defined as:

$$L^{\text{ppo},t}(\theta, \theta^t) = \frac{1}{|\mathcal{D}^t|T} \sum_{\tau \in \mathcal{D}^t} \sum_{t=0}^T \min \left( r_t^t \hat{A}_t^t, \text{clip}(r_t^t, 1 - \epsilon, 1 + \epsilon) \hat{A}_t^t \right) \quad (3)$$

$$L^{\text{ppo},s}(\theta) = \frac{1}{|\mathcal{D}^s|T} \sum_{\tau \in \mathcal{D}^s} \sum_{t=0}^T \min \left( r_t^s \hat{A}_t^s, \text{clip}(r_t^s, 1 - \epsilon, 1 + \epsilon) \hat{A}_t^s \right) \quad (4)$$

where  $\mathcal{D}^t$  and  $\mathcal{D}^s$  are sets of teacher group and student group trajectories by interacting with environment using  $E_{\theta_k^t}$ ,  $\pi_{\theta_k}$

and  $E_{\theta_k^s}$ ,  $\pi_{\theta_k}$ , respectively.  $T$  is the length of corresponding trajectory.  $r_t^t, r_t^s$  are ratio functions of two groups:

$$r_t^t(\theta, \theta^t) = \frac{\pi_{\theta}(\mathbf{a}_t^t | \mathbf{o}_t^t, E_{\theta^t}(\mathbf{s}_t^t))}{\pi_{\theta_{\text{old}}}(\mathbf{a}_t^t | \mathbf{o}_t^t, E_{\theta_{\text{old}}}(\mathbf{s}_t^t))} \quad (5)$$

$$r_t^s(\theta) = \frac{\pi_{\theta}(\mathbf{a}_t^s | \mathbf{o}_t^s, E_{\theta^s}(\mathbf{o}_{t-H:t}^s))}{\pi_{\theta_{\text{old}}}(\mathbf{a}_t^s | \mathbf{o}_t^s, E_{\theta_{\text{old}}}(\mathbf{o}_{t-H:t}^s))} \quad (6)$$

Value function  $V_{\phi}$  is trained by regression on mean-square error between  $V_{\phi}(\mathbf{s}_t, \mathbf{c}_t, \mathbf{z}_t)$  and  $\hat{R}_t$  estimated by Generalized Advantage Estimation (GAE) using trajectories from both groups. The Monte-Carlo approximation of value loss is defined as:

$$L^{\text{value}}(\phi) = \frac{1}{|\mathcal{D}|T} \sum_{\tau \in \mathcal{D}} \sum_{t=0}^T \left( V_{\phi}(\mathbf{s}_t, \mathbf{z}_t) - \hat{R}_t \right)^2 \quad (7)$$

In order to make proprioceptive encoder of student learn from privileged encoder of teacher, reconstruction loss is introduced to further update the proprioceptive encoder by minimizing the outputs difference between proprioceptive encoder and privileged encoder. Its monte carlo approximation is defined as:

$$L^{\text{rec}}(\theta^s) = \frac{1}{|\mathcal{D}^s|T} \sum_{\tau \in \mathcal{D}^s} \sum_{t=0}^T \|E_{\theta^s}(\mathbf{o}_{t-H:t}^s) - E_{\theta^t}(\mathbf{s}_t^s)\|_2^2 \quad (8)$$

---

#### Algorithm 1 Concurrent Teacher-Student Training

---

- 1: Initialize environment and networks
  - 2: **for**  $k = 0, 1, \dots$  **do**
  - 3:   Collect sets of trajectories  $\mathcal{D}_k$  with latest policy
  - 4:   Compute  $\hat{R}_t$  and  $\hat{A}_t$  using GAE
  - 5:   **for** epoch  $i = 0, 1, \dots$  **do**
  - 6:     Use  $\theta$  represent  $\theta^t, \theta$  for notational brevity
  - 7:      $\theta \leftarrow \theta + \alpha_{\text{ppo}} \nabla_{\theta} (L_i^{\text{ppo},t}(\theta) + L_i^{\text{ppo},s}(\theta))$
  - 8:      $\phi \leftarrow \phi - \alpha_{\text{ppo}} \nabla_{\phi} L_i^{\text{value}}(\phi)$
  - 9:   **end for**
  - 10:   **for** epoch  $i = 0, 1, \dots$  **do**
  - 11:      $\theta^s \leftarrow \theta^s - \alpha_{\text{ts}} \nabla_{\theta^s} L_i^{\text{rec}}(\theta^s)$
  - 12:   **end for**
  - 13: **end for**
-

TABLE II: Reward Terms

Reward Term	Equation	Weight
Lin. velocity tracking	$\exp(-4\ \mathbf{v}_{xy}^{\text{cmd}} - \mathbf{v}_{xy}\ _2^2)$	1.0
Ang. velocity tracking	$\exp(-4(\omega_z^{\text{cmd}} - \omega_z)^2)$	0.5
Lin. velocity ( $z$ )	$v_z^2$	-2.0/ <b>-0.5</b>
Ang. velocity ( $xy$ )	$\ \boldsymbol{\omega}_{xy}\ _2^2$	-0.05
Joint acceleration	$\ddot{\mathbf{q}}^2$	$-2.5 \times 10^{-7}$
Joint power	$ \boldsymbol{\tau}  \dot{\mathbf{q}} ^T$	$-2 \times 10^{-5}$
Joint Torque	$\ \boldsymbol{\tau}\ _2^2$	-0.0001
Base height	$(h^{\text{des}} - h)^2$	-1
Action rate	$\ \mathbf{a}_t - \mathbf{a}_{t-1}\ _2^2$	-0.01
Action smoothness	$\ \mathbf{a}_t - 2\mathbf{a}_{t-1} - \mathbf{a}_{t-2}\ _2^2$	-0.01
Collision	$n_{\text{collision}}$	-1
Joint limit	$n_{\text{limitation}}$	-2
Feet regulation	$r^{\text{fr}}$	-0.05
Orientation ( $xy$ )	$\ \mathbf{g}_{xy}\ _2$	<b>-5.0</b>
Feet distacne	$r^{\text{fd}}$	<b>-100</b>
Feet contact force	$r^{\text{ff}}$	<b>-2.0</b>
Feet velocity	$r^{\text{fv}}$	<b>-2.0</b>

Black: reward terms used for both biped and quadruped.

Red: biped modified weights and newly added terms.

### III. IMPLEMENTATION DETAILS

#### A. Reward Design

We employed a unified reward structure adaptable to quadruped robots of various sizes and dynamic parameters. For point-foot bipedal robot, we reused all the reward items from the quadruped system, with the addition of a minimal number of necessary reward terms tailored to its specific locomotive traits. Details of the reward function are presented in Table II.

To enable the agent to produce smooth and graceful motions, we conducted a comparative analysis on the locomotion characteristics of legged robots based on optimal control and reinforcement learning. We discovered the most significant difference lies in the end-effectors trajectories of the swing legs. The end effectors of the swing legs of legged robots based on reinforcement learning tend to move along the shortest trajectory, keeping them close to the ground throughout. This results in motions that are neither visually appealing nor well-suited for unstructured terrains. In contrast, optimal control-based approaches often plan a smooth curve so that the feet takeoff and touchdown vertically. We proposed a feet regulation reward  $r^{\text{fr}}$  to characterize this feature:

$$r^{\text{fr}} = \sum_{\text{feet}} \|\mathbf{v}_{xy}^{\text{foot}}\|_2^2 \exp\left(-\frac{p_z^{\text{foot}}}{0.025h^{\text{des}}}\right) \quad (9)$$

where  $p_z^{\text{foot}}$ ,  $\mathbf{v}^{\text{foot}}$ ,  $h^{\text{des}}$  are foot height, foot velocity and desired body height with respect to the ground, respectively.

In consideration of the higher degree of underactuation in bipeds compared to quadrupeds, maintaining base stability presents a more significant challenge. Accordingly, we have carefully decreased the penalty associated with Z-direction linear velocity. In parallel, we introduced a base orientation reward function that penalizes the roll and pitch angles of the base. This adjustment enables the bipedal robot to maintain a level posture across a variety of complex terrains as effectively as possible. Our observations indicate that the bipedal training strategy tends to favor foot placements closer to the center-line to minimize torque on the center of mass. However, this

behavior increases the risk of leg collisions. To mitigate this issue, we have incorporated a feet distance penalty function, denoted as  $r^{\text{fd}}$ :

$$r^{\text{fd}} = \max\left(0, 0.1 - \|\mathbf{p}_{xy}^{\text{left}} - \mathbf{p}_{xy}^{\text{right}}\|_2\right) \quad (10)$$

Due to the point-foot bipedal robot's lack of sole structures, it is unable to maintain static standing balance. Therefore, we referred to the method in [26] and added periodic rewards to encourage the generation of a regular trotting gait for self-balancing. The rewards  $r^{\text{ff}}$  and  $r^{\text{fv}}$  penalize the foot contact forces during the stance phase and foot velocities during the swing phase, respectively, allowing the agent to learn specified contact patterns.

$$r^{\text{ff}} = \sum_{\text{feet}} \left[1 - C_i^{\text{des}}(\phi_i)\right] \left[1 - \exp\left(-0.04 \|\mathbf{f}^{\text{foot},i}\|_2\right)\right] \quad (11)$$

$$r^{\text{fv}} = \sum_{\text{feet}} C_i^{\text{des}}(\phi_i) \left[1 - \exp\left(-4 \|\mathbf{v}_{xy}^{\text{foot},i}\|_2\right)\right] \quad (12)$$

where  $\mathbf{f}^{\text{foot},i}$  represents the ground contact force of the corresponding leg,  $i \in (\text{left}, \text{right})$ . The function  $C_i^{\text{des}}$  computes the desired foot contact state from the gait phase, following the method described in [27].

#### B. Linear Velocity Estimator

We consider the linear velocity of the base is part of privileged state  $\mathbf{s}_t$  instead of proprioceptive observations  $\mathbf{o}_t$ , due to the challenges associated with obtaining accurate and reliable velocity estimation by using proprioceptions in real-world. Quadrupedal robots have enough legs in contact with the terrain that explicit estimates of velocity are not indispensable. However, point-foot bipedal robot lacks enough contact information. This can lead to a decrease in the ability of bipedal robots to navigate complex terrain. Therefore, we adopt the method proposed in [12] and additionally integrate a velocity estimator for bipedal robots, which uses observation sequence  $\mathbf{o}_{t-H:t}^s$  to estimate base linear velocity and provide it to the policy network.

#### C. Environment Setup

We use IsaacGym simulator [28] to train 8192 parallel agents on different terrains, each group contains 4096 agents. The training process needs 3000 iterations to get capability of traversing challenging terrains, which takes about 1 hour 45 minutes of wall clock time on NVIDIA RTX 4090. But its performance will continue to improve over an extended period of training. Each episode lasts no longer than 20s, corresponding to 1,000 time steps with a control frequency of 50 Hz. Episodes were terminated upon reaching the maximum time or robot fall-over. Joint PD controller parameters are  $k_p = 20.0$ ,  $k_d = 0.5$  for A1,  $k_p = 40.0$ ,  $k_d = 1.0$  for Aliengo,  $k_p = 40.0$ ,  $k_d = 1.5$  for biped. The algorithm performed an iteration every 24 time steps. Hyper-parameters for training are presented in Table III, and adaptation of the learning rate is similar to [13].

To achieve robust locomotion in various terrain, it is crucial to implement a proper training curriculum strategy. We adopt a

TABLE III: Hyper Parameters for Training

PPO	
Batch size	$8192 \times 24$
Mini-batch size	$8192 \times 6$
Number of epochs	5
Clip range	0.2
Entropy coefficient	0.01
Discount factor	0.99
GAE discount factor	0.95
Desired KL-divergence	0.01
Learning rate	adaptive
Proprioceptive Encoder	
Batch size	$4096 \times 24$
Mini-batch size	$4096 \times 6$
Number of epochs	5
Learning rate	$1 \times 10^{-3}$

terrain curriculum similar to [13]. At the beginning of training, all robots are assigned to four terrain types with the lowest difficulty, including slopes, rough slopes, stairs, and discrete obstacles shown in Fig. 3. The robots are moved to more difficult terrains once they successfully mastering velocity tracking.

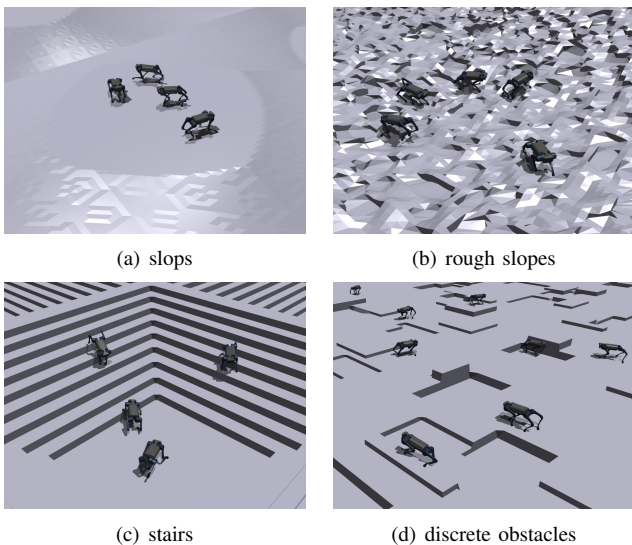


Fig. 3: Terrains in simulation

Velocity commands are uniformly and randomly sampled from a range  $[-1, 1]$ m/s at the beginning. Once they step out of the most difficult terrain and performed velocity tracking well, the velocity commands sampling range is incrementally increased to foster more agile movement skills.

To compensate for the gap between simulation and the real-world, we randomize mass of base and legs, CoM of base, the friction and restitution between the rigid body and the ground, the PD gains and motor strength and position offsets of joints, and action delay. The details of the randomization are presented in Table IV.

## IV. RESULTS

### A. Latent Space Analysis

To elucidate the acquired representations, we analyzed the structure of the latent space. We used the proprioceptive

TABLE IV: Domain Randomization

Randomization Term	Range	Unit
Link mass	$[0.8, 1.2] \times \text{nominal value}$	Kg
Payload mass	$[-1, 3]$	Kg
CoM of base	$[-7.5, 7.5] \times [-5, 5] \times [-5, 5]$	cm
Friction	$[0.2, 1.7]$	-
Restitution	$[0.25, 0.75]$	-
Joint $K_p$	$[0.8, 1.2] \times \text{nominal value}$	N-rad
Joint $K_d$	$[0.8, 1.2] \times \text{nominal value}$	N-rad/s
Action delay	$[0, 20]$	ms

encoder to obtain latent representations on different terrains (slopes, rough slopes, stairs, and discrete obstacle) in simulation, and compare the representations encoded by different robots. We conducted t-distributed stochastic neighbor embedding (t-SNE) on the latent representations for the above terrains, as shown in Fig. 4. We found that the latent representations were distributed distinctly for different terrains and thus carried sufficient information about the features of terrains. Moreover, the t-SNE plot demonstrates that quadruped robots possess a stronger capability to perceive terrain features compared to bipedal robots, as they have more legs to make contacts with the environment.

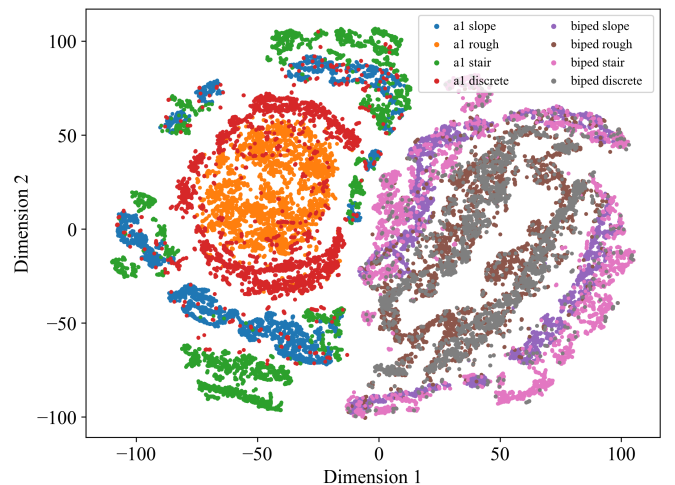


Fig. 4: The t-SNE visualization of Latent Representations from Encoder for A1 and Biped

### B. Evaluation Results

For a comparative evaluation, we compared the training results of these algorithms for the A1 robot as follows:

- Oracle: Policy full state was trained by PPO with.
- Baseline: Policy with proprioceptive encoder was trained by PPO.
- EstimatorNet: Policy was concurrently trained with an estimator network estimates body velocity and feet height similar to [12].
- Two-stages teacher-student: The proposed method trained in two stages where student policy was trained by supervised learning as original teacher-student learning framework.

For a fair comparison, all the methods above were trained under the same training configuration detailed in Section III-C,

and use the same network scale and random seeds. Our evaluations will employ the policy at the 5000th iteration. Specifically, for the two-stages teacher-student method, the policy is obtained by 3000 iterations for teacher and 2000 iterations for student.

We compared improvements in terrain level and tracking reward during the training process. The results are shown in Fig. 5, in which the curves are averaged over 5 seeds. The shaded area represents the standard deviation across seeds. The Baseline and EstimatorNet models exhibit comparable capabilities in traversing varied terrains and similar training velocities. However, the Baseline shows significant variability with different random seeds. Oracle model with access to privileged information achieves the highest training velocity. In the later stages of training, to minimize collisions and other penalties for higher discounted returns, it slightly compromises command tracking under specific conditions, as indicated by a minor decline in the terrain level on the graph. The training velocity of our teacher model is marginally slower than that of the Oracle, and the student model lags slightly behind the teacher. Nevertheless, both eventually attain equivalent capabilities.

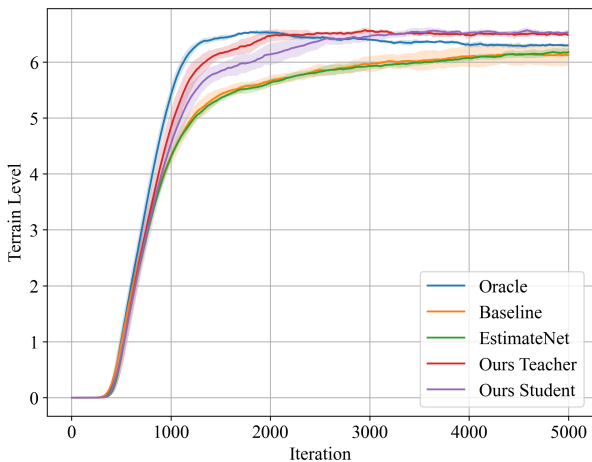


Fig. 5: Learning curves of average terrain level.

We evaluated the velocity tracking performance in simulation under various terrain conditions by distributing 8192 robots evenly among four types of terrains. Linear velocity commands were uniformly sampled from  $[-1.0, 1.0]$  m/s. Tracking errors are quantified using the norms  $\|v_{xy}^{cmd} - v_{xy}\|_2$ . To minimize the impact of randomness during the training process, the results presented in the Table V are the average outcomes of policies trained with five different seeds. It shows that the tracking capability of our method outperforms the other methods on all terrains.

TABLE V: Velocity Tracking Error

Method	Slope	Rough	Stairs	Obstacles
Baseline	0.119	0.165	0.195	0.132
EstimatorNet	0.111	0.158	0.193	0.125
Two-stages teacher-student	0.103	0.141	0.138	0.113
Ours	<b>0.098</b>	<b>0.128</b>	<b>0.133</b>	<b>0.105</b>

To evaluate the robustness of policy, we perturbed robots in

the simulation under various terrains by applying random force to the robot’s body and record their survival rates. Specifically, the direction of the push was chosen randomly, with the applied force inducing a velocity change of approximately 2m/s of the robots. Results in Table VI show that our method is more robust in challenging terrains.

TABLE VI: Push Survival Rate in %

Method	Slope	Rough	Stairs	Obstacles
Baseline	<b>97.13</b>	93.78	94.72	95.29
EstimatorNet	95.83	93.21	94.05	95.01
Two-stages teacher-student	96.86	94.04	94.87	<b>95.92</b>
Ours	96.34	<b>94.50</b>	<b>95.24</b>	95.58



Fig. 6: Aliengo steps over a moving platform

### C. Real-World Experiments

We implemented the student policy on quadruped robots of varying sizes, including the Unitree A1 and Aliengo, as well as on the more challenging point-foot bipedal robot, LimX Dynamics P1. All demonstrated exceptional robustness and terrain traversal capabilities, validating the universality and superior performance of our method.

Fig. 6 shows the quadruped robot is engaged in a complex interaction with a moving platform, providing a clear illustration of its robustness against uncertainty and terrain adaptability. Initially, the robot maintains regular walking towards the platform. When the robot’s left front leg encounters an obstacle, it instinctively retracts and lifts to step onto the platform, a response not explicitly trained for since the stairs used during training did not feature gaps. This behavior demonstrates the robot’s generalization capabilities, allowing it to adapt to new environmental challenges despite the absence of direct prior experience with such specific scenarios. Once the left front leg secures placement on the platform, the robot is able to discern the platform’s elevation, thereby enabling the right front leg to accurately follow suit and step onto the platform without undesirable collision.

As the platform commences sliding upon the robot’s ascent, the robot reacts to this motion. Its hind legs promptly engage, adjusting to maintain balance in response to the new dynamics introduced by the moving platform. This demonstrates the robot’s reactive balance capabilities and its proficiency in stabilizing itself amid changing environmental conditions. As the robot descends from the platform, the placement of its left hind leg is dynamically adjusted in relation to the robot’s

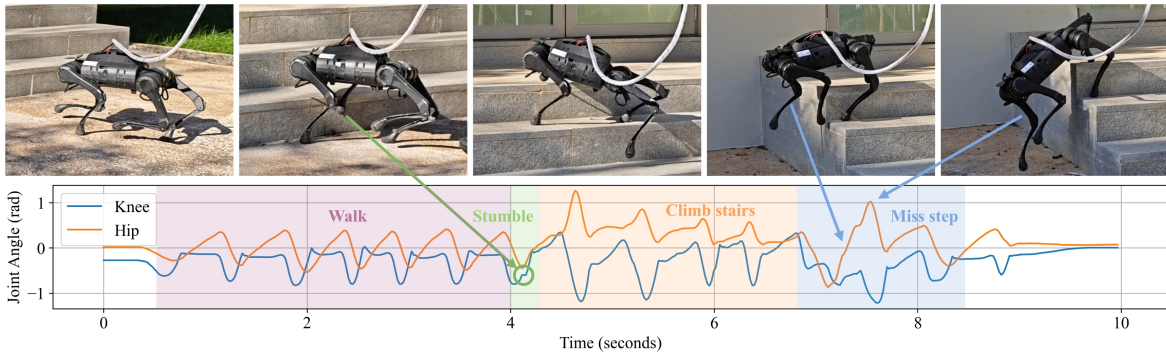


Fig. 7: A1 locomotion with stairs and missing step adaptation

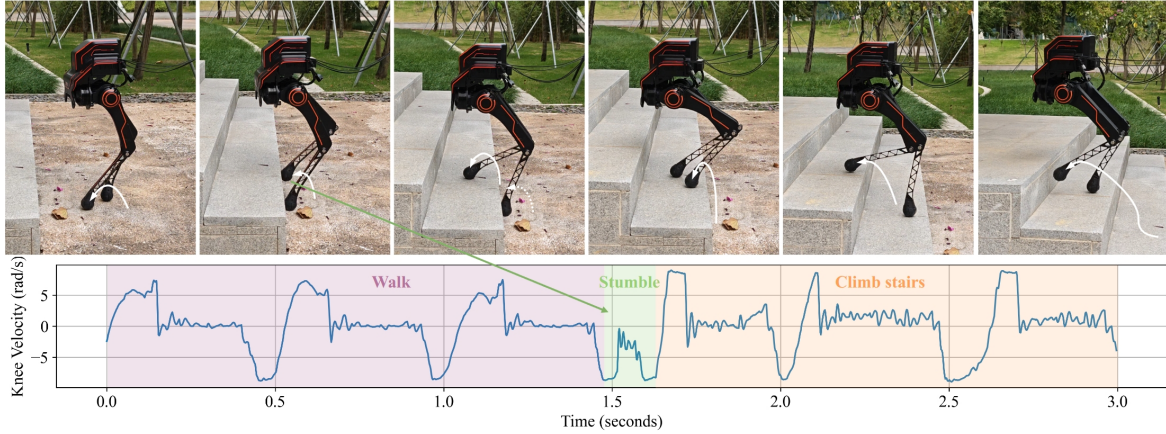


Fig. 8: Biped locomotion with stairs

overall posture and the positioning of its other legs. During its swing phase, it selects a more forward foothold to align with the robot’s overarching motion, resulting in an S-shaped swing trajectory.

Fig. 7 provided visual and data analysis illustrates quadruped robot’s motion as it encounters stairs and missing step. When the robot encounters a step while walking, its right front leg is quickly lifted after being stumbled, allowing it to step onto the stair. The robot then smoothly reaches the top and proceeds toward the edge until its front leg steps into empty space, initiating a fall. Immediately sensing the change in terrain, the robot reacts swiftly, extending its front legs to seek additional support and keeping its center of mass within a safe zone determined by the stance of its limbs. Once the front legs make contact, the hind legs follow, enabling the robot to safely return to the ground.

Fig. 8 demonstrates the effectiveness of our policy applied to a more challenging bipedal platform. The policy enables the robot to maintain stable forward locomotion on flat surfaces. When the right leg strikes the edge of the stair, the velocity of the knee joint rapidly drops to zero to prevent loss of balance due to inertia, and lifts upwards to navigate over the obstacle of the stair. Then, when the left leg ascends the stair, the robot briefly adopts a double-support stance to secure its base stability. After perceiving the height of the initial step, the biped transitions to the next level smoothly, avoiding collisions and demonstrating effective stair-climbing.

## V. CONCLUSION

In this study, we present the Concurrent Teacher-Student Learning framework, designed to equip legged robots with the capability to navigate unstructured terrains using purely proprioception. The effectiveness of this framework has been validated through its implementation on differently sized quadruped robots, showcasing their ability to maneuver over moving platforms and stairs. Even for bipedal robots with completely different configurations and higher degrees of underactuation, the strategies trained through our method also achieve excellent robustness and terrain traversal capabilities. A notable limitation of this approach is the requirement for physical leg-obstacle interaction for adaptation. Future efforts will focus on incorporating exteroceptive inputs into the locomotion system, aiming to refine gait planning and obstacle negotiation strategies before physical contact occurs.

## REFERENCES

- [1] M. Hutter, C. Gehring, D. Jud, A. Lauber, C. D. Bellicoso, V. Tsounis, J. Hwangbo, K. Bodie, P. Fankhauser, M. Bloesch, R. Diethelm, S. Bachmann, A. Melzer, and M. Hoepflinger, “Anymal - a highly mobile and dynamic quadrupedal robot,” in *2016 IEEE/RSJ International Conference on Intelligent Robots and Systems (IROS)*, 2016, pp. 38–44.
- [2] C. Gehring, P. Fankhauser, L. Isler, R. Diethelm, S. Bachmann, M. Potz, L. Gerstenberg, and M. Hutter, “Anymal in the field: Solving industrial inspection of an offshore hvdc platform with a quadrupedal robot,” in *Field and Service Robotics*, G. Ishigami and K. Yoshida, Eds. Singapore: Springer Singapore, 2021, pp. 247–260.

- [3] Y.-H. Shin, S. Hong, S. Woo, J. Choe, H. Son, G. Kim, J.-H. Kim, K. Lee, J. Hwangbo, and H.-W. Park, "Design of kaist hound, a quadruped robot platform for fast and efficient locomotion with mixed-integer nonlinear optimization of a gear train," in *2022 International Conference on Robotics and Automation (ICRA)*, 2022, pp. 6614–6620.
- [4] G. Bledt, M. J. Powell, B. Katz, J. Di Carlo, P. M. Wensing, and S. Kim, "Mit cheetah 3: Design and control of a robust, dynamic quadruped robot," in *2018 IEEE/RSJ International Conference on Intelligent Robots and Systems (IROS)*, 2018, pp. 2245–2252.
- [5] B. Katz, J. D. Carlo, and S. Kim, "Mini cheetah: A platform for pushing the limits of dynamic quadruped control," in *2019 International Conference on Robotics and Automation (ICRA)*, 2019, pp. 6295–6301.
- [6] Y. Gong, R. Hartley, X. Da, A. Hereid, O. Harib, J.-K. Huang, and J. Grizzle, "Feedback control of a cassie bipedal robot: Walking, standing, and riding a segway," in *2019 American Control Conference (ACC)*. IEEE, 2019, pp. 4559–4566.
- [7] Z. Hong, H. Chen, and W. Zhang, "Three-dimensional dynamic running with a point-foot biped based on differentially flat slip," in *2022 IEEE/RSJ International Conference on Intelligent Robots and Systems (IROS)*. IEEE, 2022, pp. 1169–1174.
- [8] P. M. Wensing, M. Posa, Y. Hu, A. Escande, N. Mansard, and A. D. Prete, "Optimization-based control for dynamic legged robots," *IEEE Transactions on Robotics*, vol. 40, pp. 43–63, 2024.
- [9] J. Hwangbo, J. Lee, A. Dosovitskiy, D. Bellicoso, V. Tsounis, V. Koltun, and M. Hutter, "Learning agile and dynamic motor skills for legged robots," *Science Robotics*, vol. 4, no. 26, p. eaau5872, 2019. [Online]. Available: <https://www.science.org/doi/abs/10.1126/scirobotics.aau5872>
- [10] A. Kumar, Z. Fu, D. Pathak, and J. Malik, "RMA: Rapid Motor Adaptation for Legged Robots," in *Proceedings of Robotics: Science and Systems*, Virtual, July 2021.
- [11] G. B. Margolis, G. Yang, K. Paigwar, T. Chen, and P. Agrawal, "Rapid locomotion via reinforcement learning," *The International Journal of Robotics Research*, vol. 43, no. 4, pp. 572–587, 2024.
- [12] G. Ji, J. Mun, H. Kim, and J. Hwangbo, "Concurrent training of a control policy and a state estimator for dynamic and robust legged locomotion," *IEEE Robotics and Automation Letters*, vol. 7, no. 2, pp. 4630–4637, 2022.
- [13] N. Rudin, D. Hoeller, P. Reist, and M. Hutter, "Learning to walk in minutes using massively parallel deep reinforcement learning," in *Proceedings of the 5th Conference on Robot Learning*, ser. Proceedings of Machine Learning Research, A. Faust, D. Hsu, and G. Neumann, Eds., vol. 164. PMLR, 08–11 Nov 2022, pp. 91–100. [Online]. Available: <https://proceedings.mlr.press/v164/rudin22a.html>
- [14] J. Lee, J. Hwangbo, L. Wellhausen, V. Koltun, and M. Hutter, "Learning quadrupedal locomotion over challenging terrain," *Science Robotics*, vol. 5, no. 47, p. eabc5986, 2020. [Online]. Available: <https://www.science.org/doi/abs/10.1126/scirobotics.abc5986>
- [15] J. Wu, G. Xin, C. Qi, and Y. Xue, "Learning robust and agile legged locomotion using adversarial motion priors," *IEEE Robotics and Automation Letters*, vol. 8, no. 8, pp. 4975–4982, 2023.
- [16] W. Wei, Z. Wang, A. Xie, J. Wu, R. Xiong, and Q. Zhu, "Learning gait-conditioned bipedal locomotion with motor adaptation\*," in *2023 IEEE-RAS 22nd International Conference on Humanoid Robots (Humanoids)*, 2023, pp. 1–7.
- [17] T. Miki, J. Lee, J. Hwangbo, L. Wellhausen, V. Koltun, and M. Hutter, "Learning robust perceptive locomotion for quadrupedal robots in the wild," *Science Robotics*, vol. 7, no. 62, p. eabk2822, 2022. [Online]. Available: <https://www.science.org/doi/abs/10.1126/scirobotics.abk2822>
- [18] A. Agarwal, A. Kumar, J. Malik, and D. Pathak, "Legged locomotion in challenging terrains using egocentric vision," in *6th Annual Conference on Robot Learning*, 2022.
- [19] D. Hoeller, N. Rudin, D. Sako, and M. Hutter, "Anymal parkour: Learning agile navigation for quadrupedal robots," *Science Robotics*, vol. 9, no. 88, p. eadi7566, 2024. [Online]. Available: <https://www.science.org/doi/abs/10.1126/scirobotics.adi7566>
- [20] Z. Zhuang, Z. Fu, J. Wang, C. G. Atkeson, S. Schwertfeger, C. Finn, and H. Zhao, "Robot parkour learning," in *Proceedings of The 7th Conference on Robot Learning*, ser. Proceedings of Machine Learning Research, J. Tan, M. Toussaint, and K. Darvish, Eds., vol. 229. PMLR, 06–09 Nov 2023, pp. 73–92. [Online]. Available: <https://proceedings.mlr.press/v229/zhuang23a.html>
- [21] X. Cheng, K. Shi, A. Agarwal, and D. Pathak, "Extreme parkour with legged robots," 2023.
- [22] I. M. Aswin Nahrendra, B. Yu, and H. Myung, "Dreamwaq: Learning robust quadrupedal locomotion with implicit terrain imagination via deep reinforcement learning," in *2023 IEEE International Conference on Robotics and Automation (ICRA)*, 2023, pp. 5078–5084.
- [23] J. Long, Z. Wang, Q. Li, J. Gao, L. Cao, and J. Pang, "Hybrid internal model: Learning agile legged locomotion with simulated robot response," 2024.
- [24] J. Siekmann, S. Valluri, J. Dao, F. Bermillo, H. Duan, A. Fern, and J. Hurst, "Learning Memory-Based Control for Human-Scale Bipedal Locomotion," in *Proceedings of Robotics: Science and Systems*, Corvallis, Oregon, USA, July 2020.
- [25] J. Siekmann, K. Green, J. Warila, A. Fern, and J. Hurst, "Blind Bipedal Stair Traversal via Sim-to-Real Reinforcement Learning," in *Proceedings of Robotics: Science and Systems*, Virtual, July 2021.
- [26] J. Siekmann, Y. Godse, A. Fern, and J. Hurst, "Sim-to-real learning of all common bipedal gaits via periodic reward composition," in *2021 IEEE International Conference on Robotics and Automation (ICRA)*. IEEE, 2021, pp. 7309–7315.
- [27] J. Wu, Y. Xue, and C. Qi, "Learning multiple gaits within latent space for quadruped robots," 2023.
- [28] V. Makoviychuk, L. Wawrzyniak, Y. Guo, M. Lu, K. Storey, M. Macklin, D. Hoeller, N. Rudin, A. Allshire, A. Handa, and G. State, "Isaac gym: High performance GPU based physics simulation for robot learning," in *Thirty-fifth Conference on Neural Information Processing Systems Datasets and Benchmarks Track (Round 2)*, 2021.